

Electronic Supplementary Information for

**Carbon black nanoparticle trapping: A strategy to realize the true energy storage potential
of redox-active conjugated microporous polymers**

Chang Wan Kang,^a Yoon-Joo Ko,^b Sang Moon Lee,^c Hae Jin Kim,^c Jaewon Choi,^{*d} and Seung Uk Son^{*a}

^a Department of Chemistry, Sungkyunkwan University, Suwon 16419, Korea

E-mail: sson@skku.edu

^b Laboratory of Nuclear Magnetic Resonance, National Center of Inter-University Research Facilities (NCIRF), Seoul National University, Seoul 08826, Korea

^c Korea Basic Science Institute, Daejeon 34133, Korea

^d Department of Chemistry and Research Institute of Natural Science,
Gyeongsang National University, Jinju 52828, Korea

E-mail: cjh0910@gnu.ac.kr

Fig. S1. SEM images of CB, CB@CMP-DMBs, CMP-DMB, CB-O, CB@CMP-BQs, and CMP-BQ.

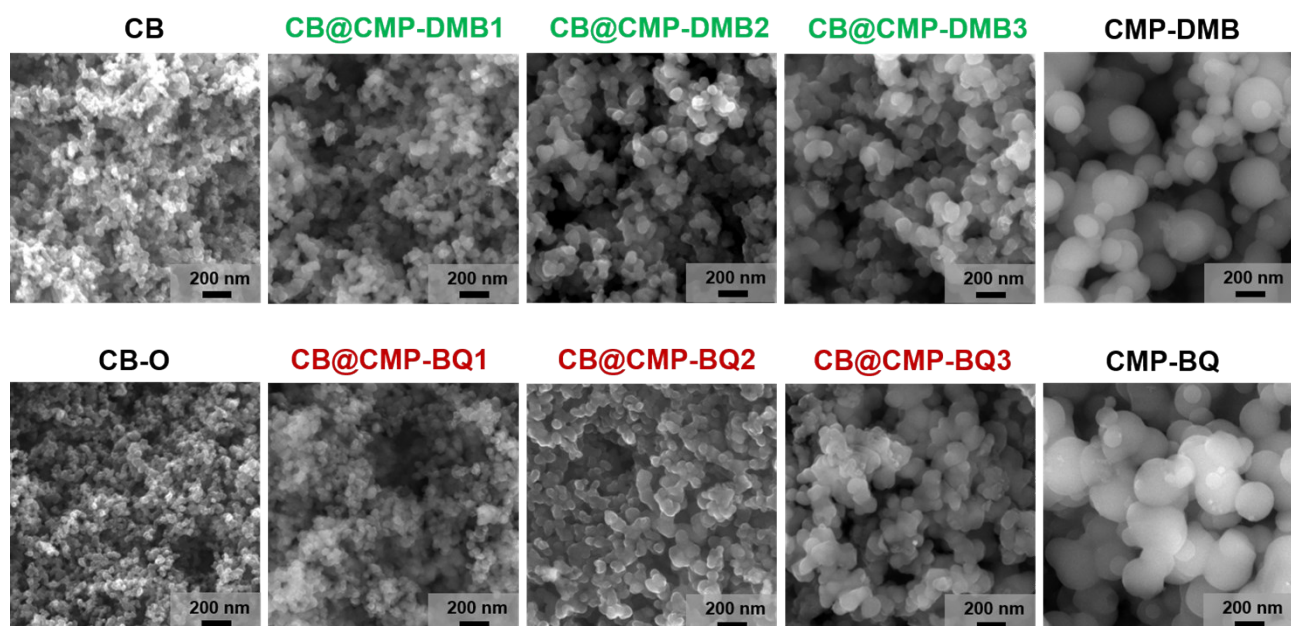


Fig. S2. TEM images of CB@CMP-DMB1, CB@CMP-DMB2, CB@CMP-BQ1, and CB@CMP-BQ2, compared with those of CB, CB@CMP-DMB3, CMP-DMB, CB-O, CB@CMP-BQ3, and CMP-BQ.

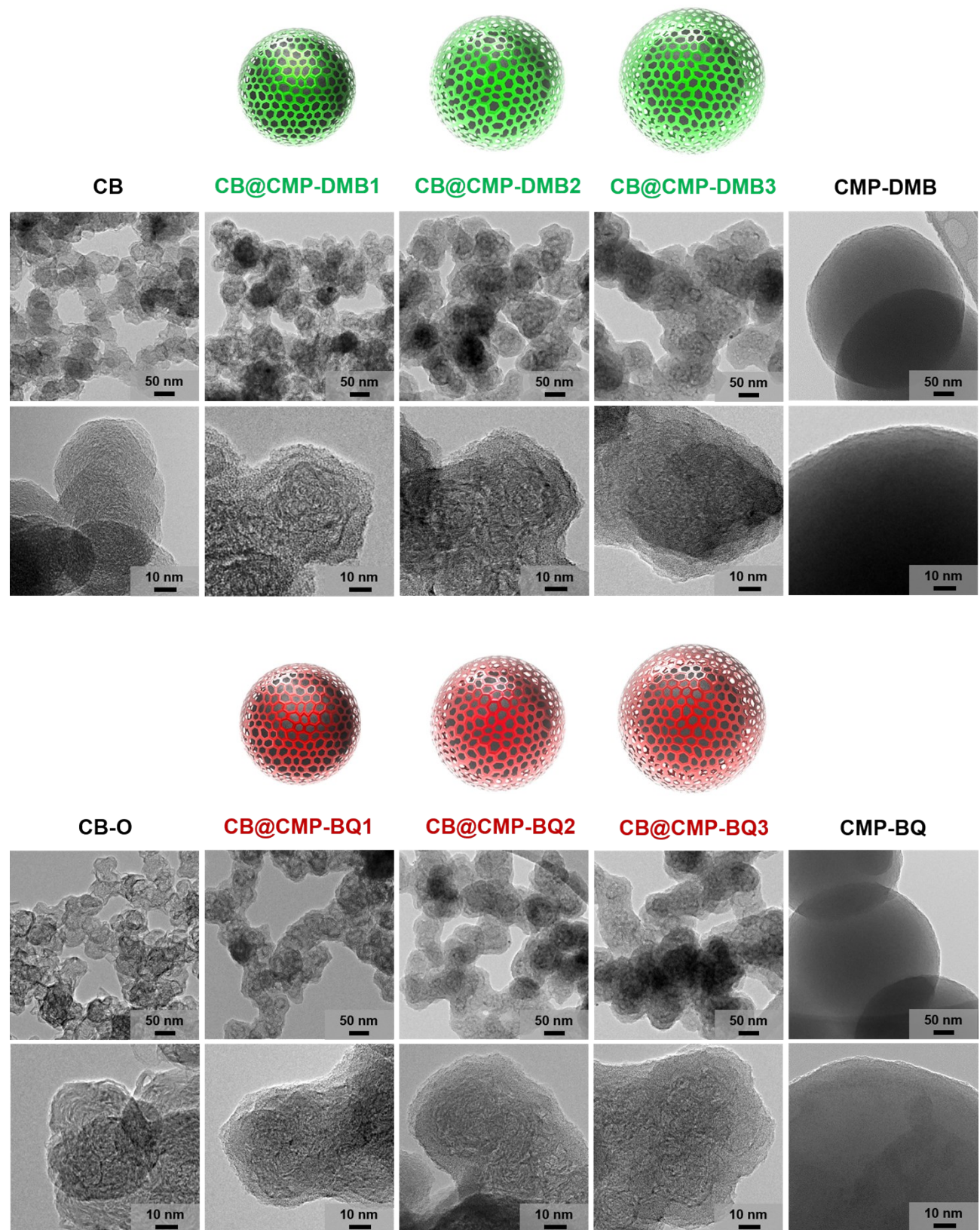


Fig. S3. TEM images of a mixture of CMP-DMB and CB@CMP-DMB that prepared by the Sonogashira coupling of 1,3,5-triethynylbenzene (0.13 mmol) and 1,4-diodo-2,5-dimethoxybenzene (0.20 mmol) in the presence of CB (12.5 mg).

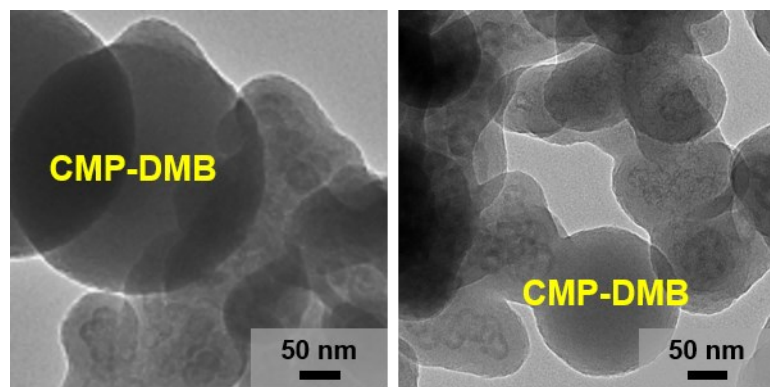


Fig. S4. N₂ adsorption-desorption isotherm curves (obtained at 77K) and pore size distribution diagrams (based on the DFT method) of CB@CMP-DMB1, CB@CMP-DMB2, CB@CMP-BQ1, and CB@CMP-BQ2.

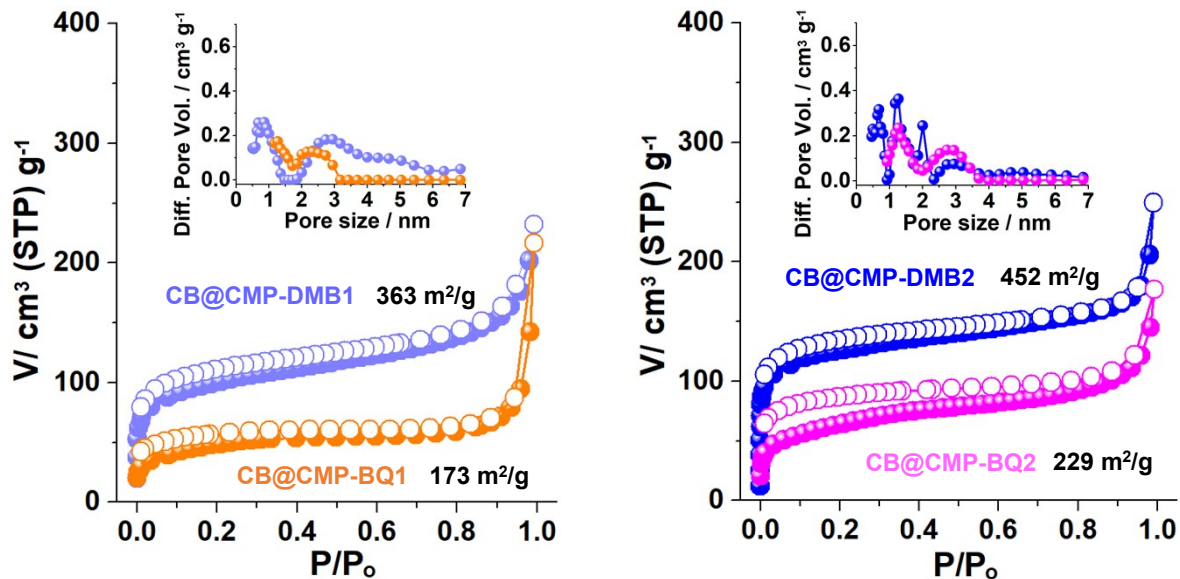


Fig. S5. IR spectra of CB@CMP-DMB1, CB@CMP-DMB2, CB@CMP-BQ1, and CB@CMP-BQ2.

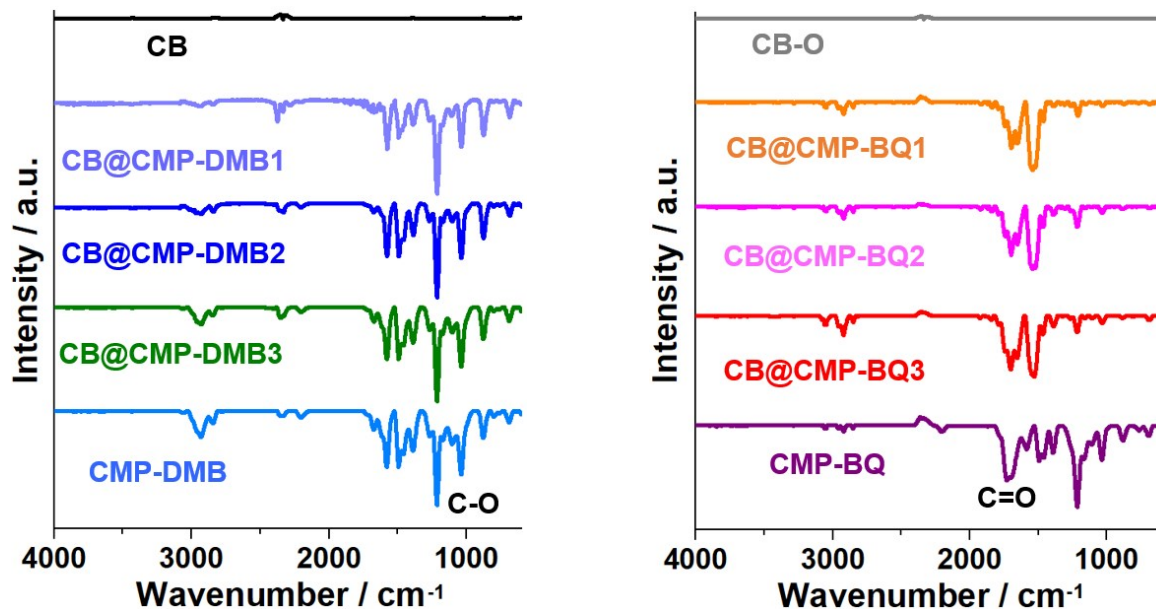


Fig. S6. Solid state ^{13}C NMR spectra of CB@CMP-DMB1, CB@CMP-DMB2, CB@CMP-BQ1, and CB@CMP-BQ2.

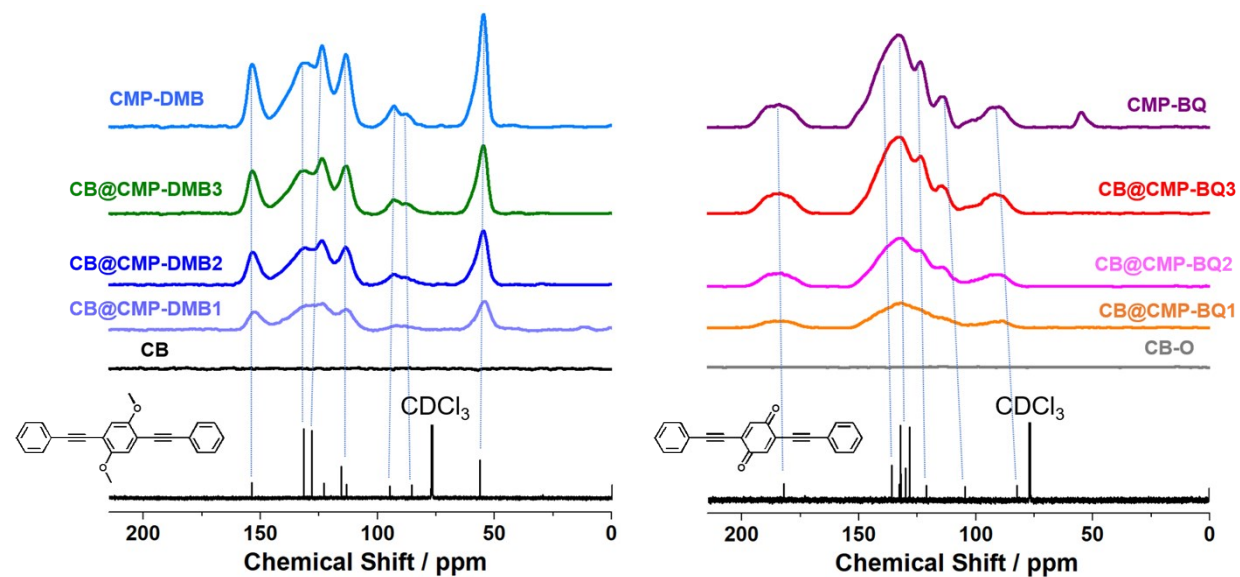


Fig. S7. PXRD patterns of CB@CMP-DMBs, CB@CMP-BQs, CMP-DMB, CMP-BQ, CB, and CB-O.

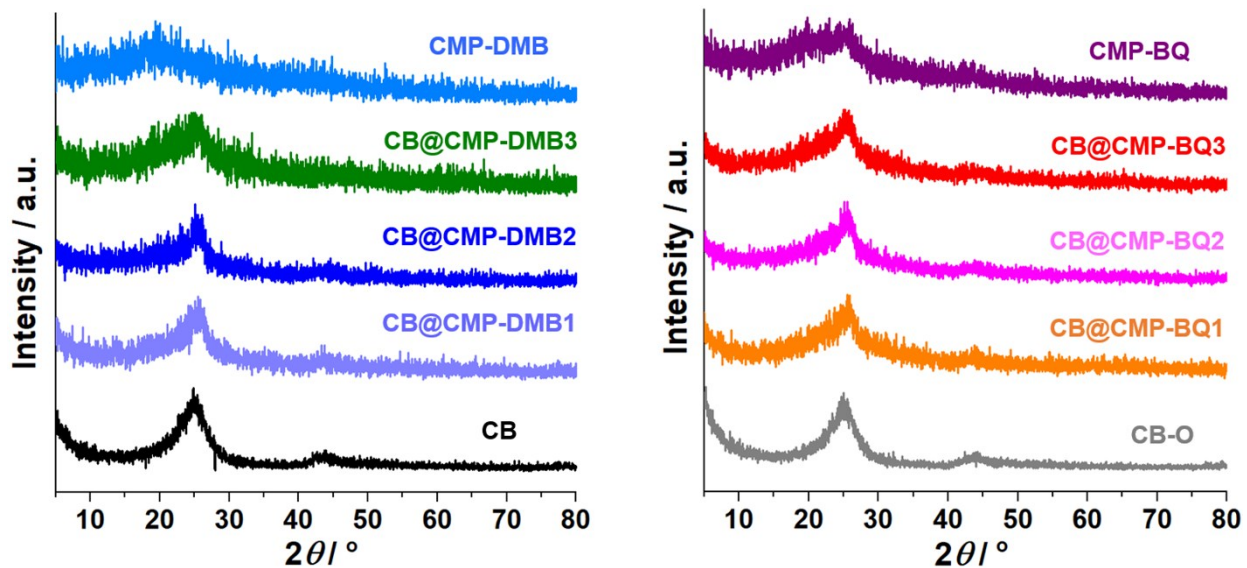


Fig. S8. TGA curves of CB@CMP-DMBs, CB@CMP-BQs, CMP-DMB, and CMP-BQ.

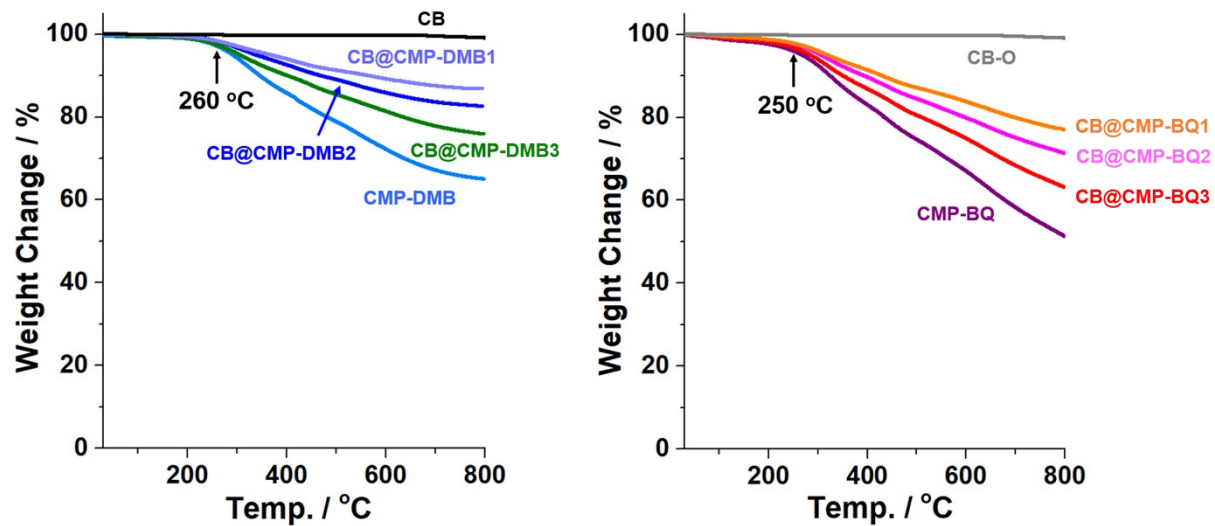


Fig. S9. (a) Cyclic voltammograms and (b) charge-discharge profiles of CB@CMP-BQ1 and CB@CMP-BQ2.

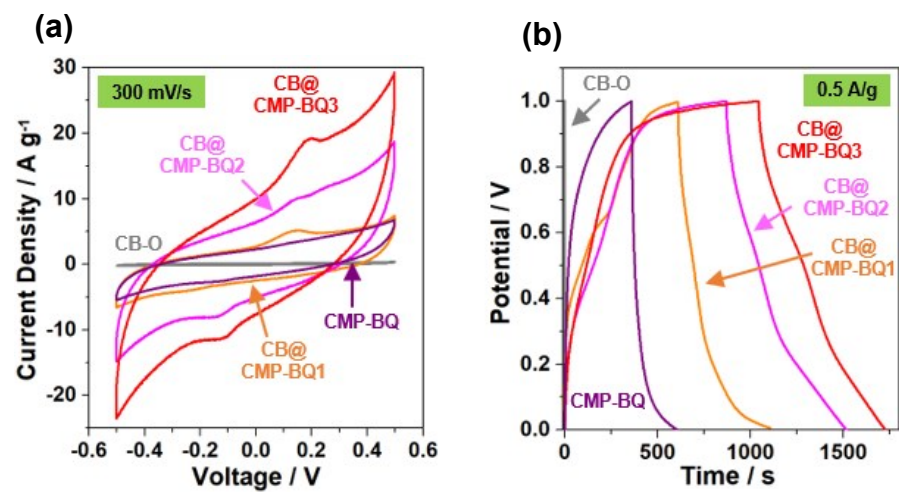


Fig. S10. Scan rate-dependent cyclic voltammograms of CB@CMP-BQ1, CB@CMP-BQ2, CB@CMP-BQ3, CB-O, and CMP-BQ.

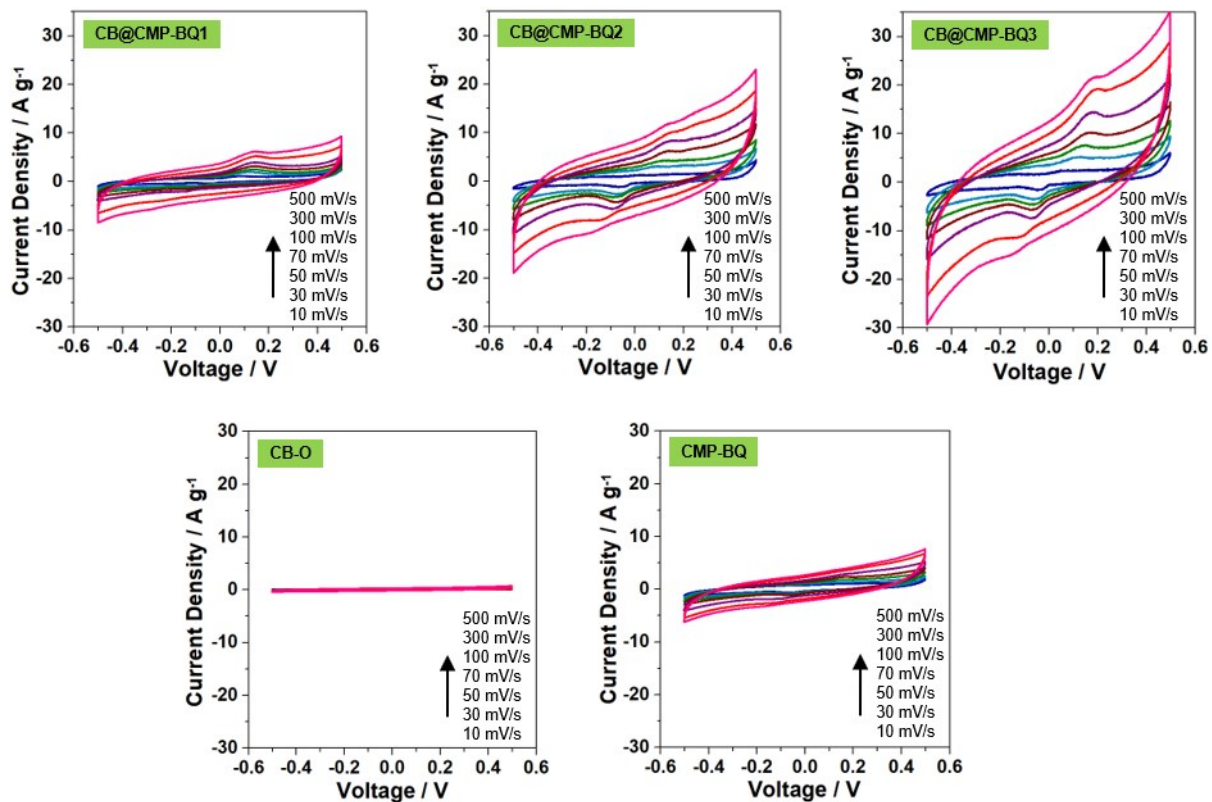


Fig. S11. Current density-dependent charge-discharge profiles of CB@CMP-BQ1, CB@CMP-BQ2, CB@CMP-BQ3, CB-O, and CMP-BQ.

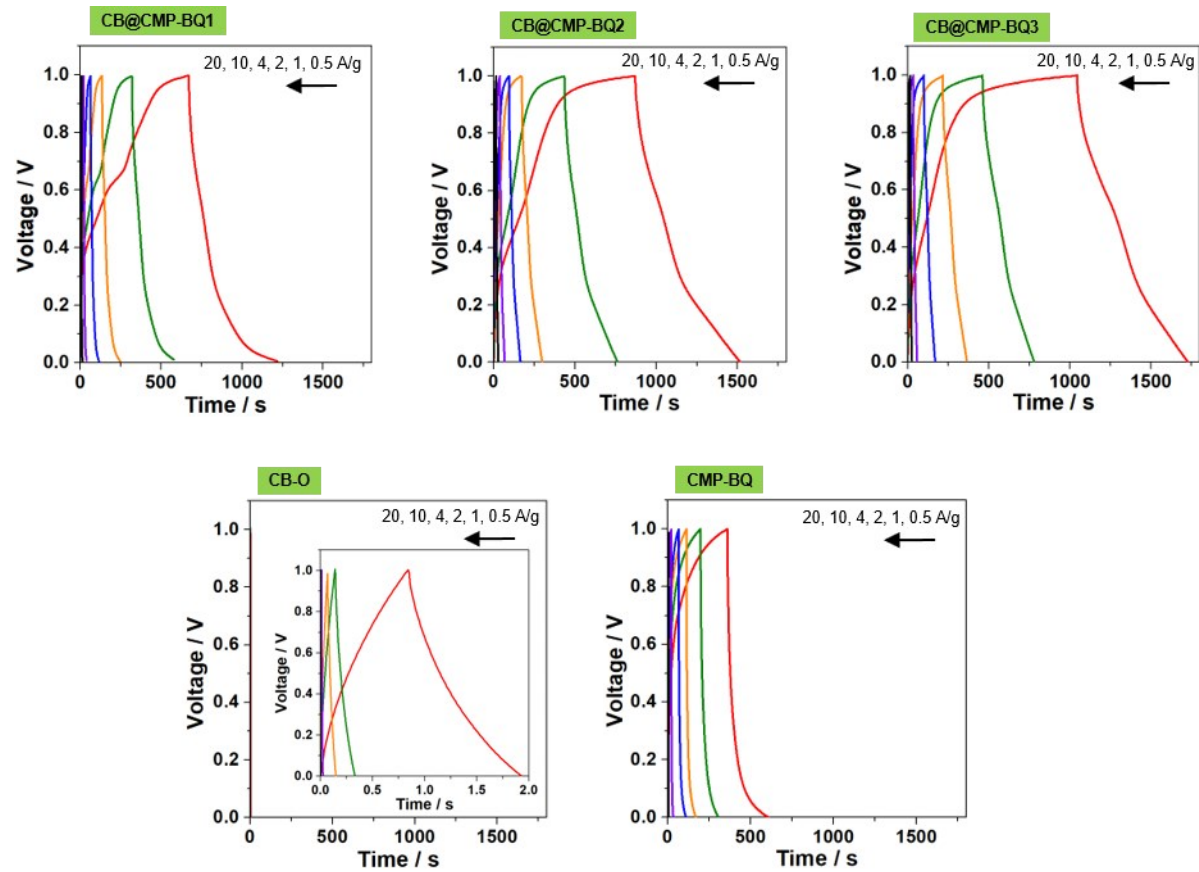


Fig. S12. (a) An equivalent circuit model used for the analysis of EIS results, (b) the fitted Nyquist plots, (c) equivalent circuit parameters of CB-O, CB@CMP-BQs, and CMP-BQ.

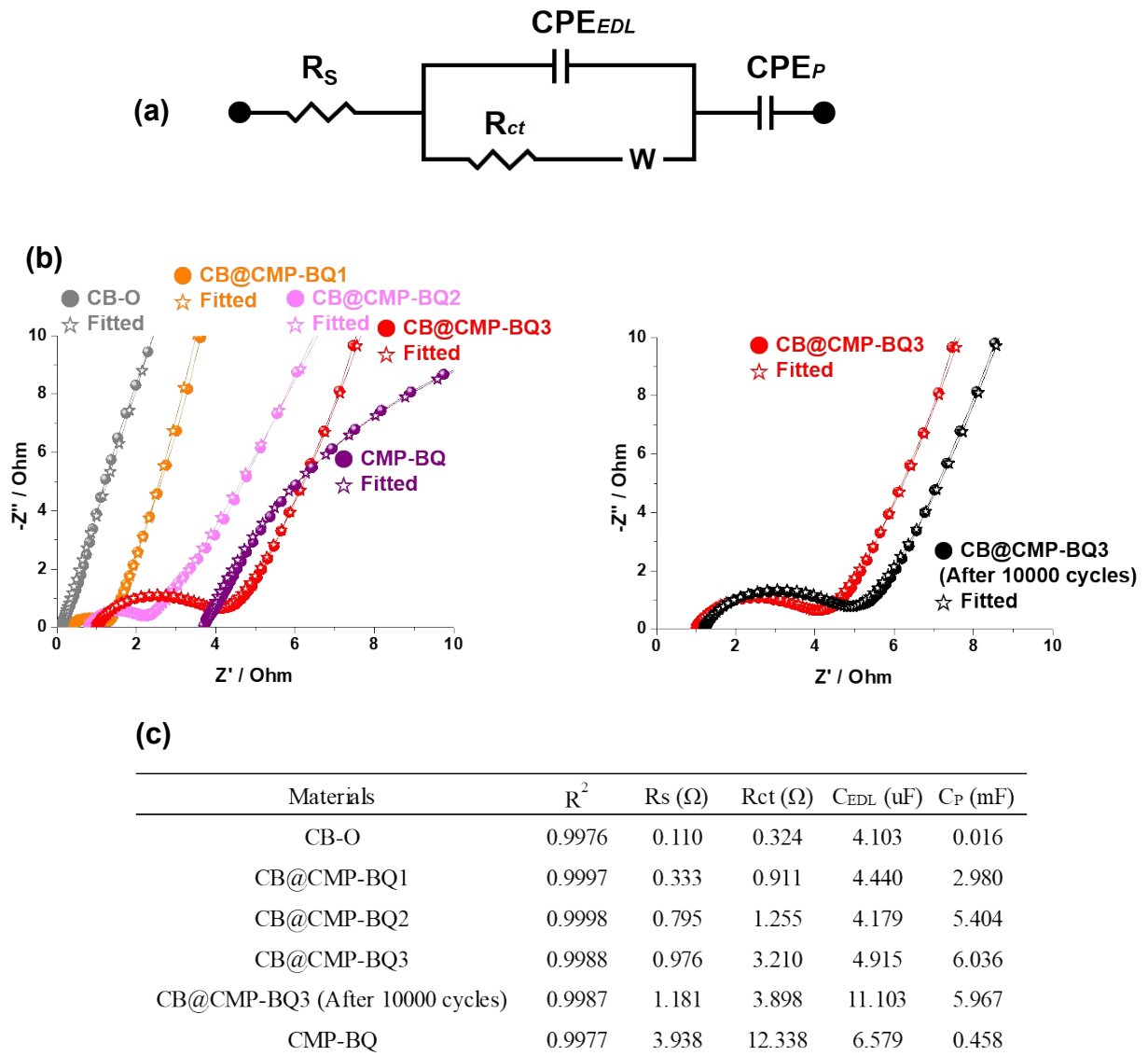


Fig. S13. (a) Photographs of pellets and (b) conductivity measurements of CB-O, CB@CMP-BQs, and CMP-BQ.



(b)

Materials	CMP-BQ	CB@CMP-BQ3	CB@CMP-BQ2	CB@CMP-BQ1	CB-O
Average Sheet Resistance (Ohm/sq)	null	25.27	15.20	9.22	6.41
Thickness (mm)	0.20	0.21	0.22	0.20	0.20
Conductivity (S/m)	null	190	300	540	780

Fig. S14. IR spectra of CB@CMP-BQ3 before and after 10000 cycles.

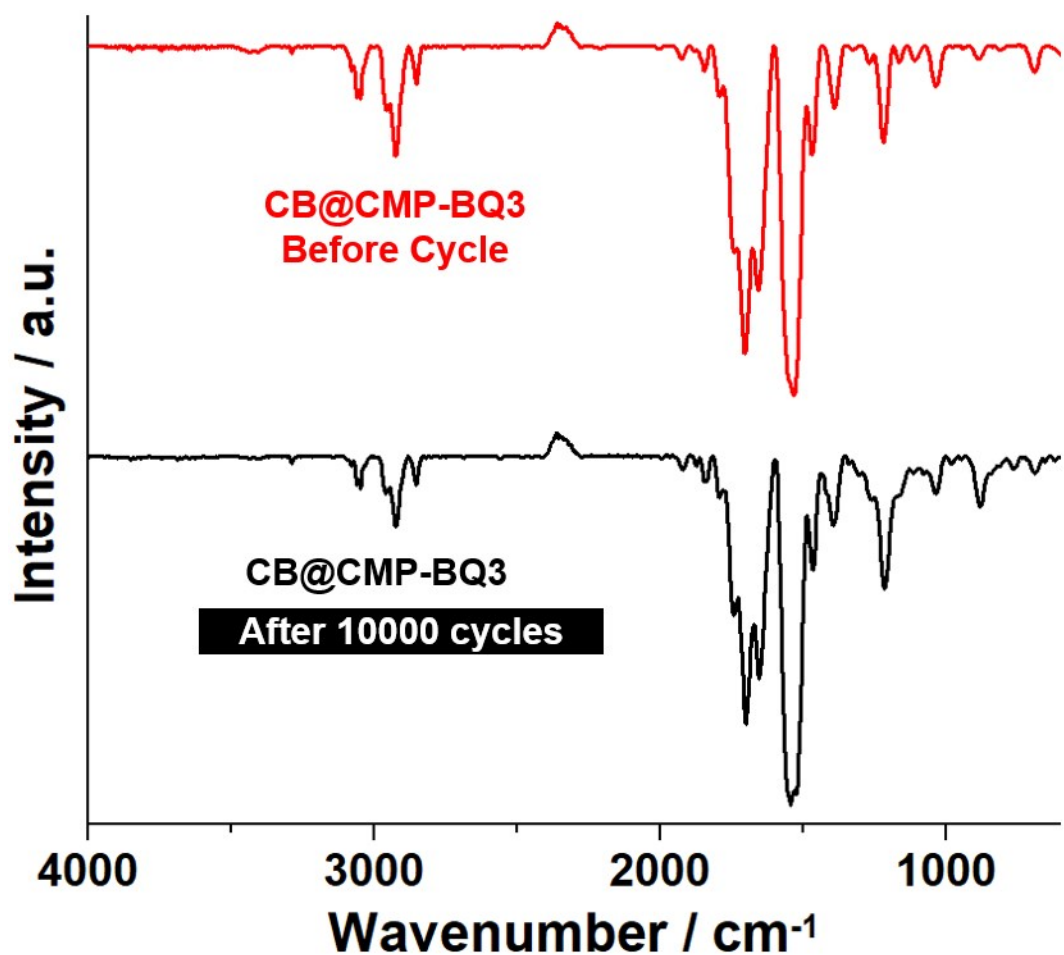


Table S1. Porous parameters of CB, CB-O, CMP-DMB, CMP-BQ, CB@CMP-DMBs, and CB@CMP-BQs.

Entry	Materials	S_{BET} ^a	V_{mic} ^b
		(m ² /g)	(cm ³ /g)
1	CB	68	0.00
2	CB@CMP-DMB1	363	0.07
3	CB@CMP-DMB2	452	0.13
4	CB@CMP-DMB3	524	0.15
5	CMP-DMB	609	0.16
6	CB-O	78	0.00
7	CB@CMP-BQ1	173	0.02
8	CB@CMP-BQ2	229	0.02
9	CB@CMP-BQ3	301	0.07
10	CMP-BQ	313	0.07

^a Surface areas based on BET theory. ^b Micropore volumes based on t-plot.

Table S2. Electrochemical performance of the recent CMP-based electrode materials for supercapacitors.

Entry	Materials	Type of Materials	Specific Capacitances (F/g)							Measurment Type	Ref
			Current Density (A/g)								
			0.1	0.2	0.5	1	2	5	10		
1	Aza-CMP@350	CMP				461		397	378	three electrode	1
2	CMP	CMP					142			three electrode	2
3	aG-PTEPE-TBPE-C	CMP/C composite		179						three electrode	3
4	TpDAB	CMP				400				three electrode	4
5	N3-CMP-1	Carbonization	175			164		149		three electrode	5
6	G-TEPA-TPA-C	Carbonization		268						two electrode	6
7	NPCM-1	Carbonization	264							two electrode	7
8	TAT-CMP-2	CMP			183	173	158	137		three electrode	8
9	Fc-GMP	CMP/C composite		231				134		two electrode	9
10	H-CMP-BPPB	CMP		220	193			120		two electrode	10
11	PAQTA	CMP			168					two electrode	11
12	H-NCB-900	Carbonization		286			224			two electrode	12
13	POP _M -TFP	POP		178	137.4	130.5				three electrode	13
	POP _M -TFP	POP		91.7						two electrode	
14	N-CMP-BZ	CMP			189			138		two electrode	14
15	GT-POP-1	CMP		324						two electrode	15
16	CB@CMP-BQ3	CMP/C composite		424	373			280		two electrode	This work

S1 Y. Kou, Y. Xu, Z. Guo and D. Jiang, *Angew. Chem. Int. Ed.* 2011, **50**, 8753-8757.S2 H. Zhang, Y. Zhang, C. Gu and Y. Ma, *Adv. Energy Mater.* 2015, **5**, 1402175.S3 K. Yuan, P. Guo-Wang, T. Hu, L. Shi, R. Zeng, M. Forster, T. Pichler, Y. Chen and U. Scherf, *Chem. Mater.* 2015, **27**, 7403-7411.S4 B. C. Patra, S. Khilari, L. Satyanarayana, D. Pradhan and A. Bhaumik, *Chem. Commun.* 2016, **52**, 7592-7595.S5 J. -S. M. Lee, T. -H. Wu, B. M. Alston, M. E. Briggs, T. Hasell, C. C. Hu and A. I. Cooper, *J. Mater. Chem. A* 2016, **4**, 7665-7673.S6 K. Yuan, T. Hu, Y. Xu, R. Graf, G. Brunklaus, M. Forster, Y. Chen and U. Scherf, *ChemElectroChem* 2016, **3**, 822-828.S7 Y. Xu, S. Wu, S. Ren, J. Ji, Y. Yue and J. Shen, *RSC Adv.* 2017, **7**, 32496-32501.S8 X. -C. Li, Y. Zhang, C. -Y. Wang, Y. Wan, W. -Y. Lai, H. Pang and W. Huang, *Chem. Sci.* 2017, **8**, 2959-2965.S9 A. M. Khattak, H. Sin, Z. A. Ghazi, X. He, B. Liang, N. A. Khan, H. R. Alanagh, A. Iqbal, L. Li and Z. Tang, *J. Mater. Chem. A* 2018, **6**, 18827-18832.S10 J. Choi, J. H. Ko, C. W. Kang, S. M. Lee, H. J. Kim, Y. -J. Ko, M. Yang and S. U. Son, *J. Mater. Chem.* 2018, **6**, 6233-6237.S11 Y. Liao, H. Wang, M. Zhu and A. Thomas, *Adv. Mater.* 2018, **30**, 1705710.S12 J. Lee, J. Choi, D. Kang, Y. Myung, S. M. Lee, H. J. Kim, Y. -J. Ko, S. -K. Kim and S. U. Son, *ACS Sustainable Chem. Eng* 2018, **6**, 3525-3532.S13 L. Xu, R. Liu, F. Wang, S. Yan, X. Shi and J. Yang, *RSC Adv.* 2019, **9**, 1586-1590.S14 S. Y. Park, C. W. Kang, S. M. Lee, H. J. Kim, Y. -J. Ko, J. Choi and S. U. Son, *Chem. Eur. J.* 2020, **26**, 12343-12348.S15 H. Zhang, X. Tang and C. Gu, *J. Mater. Chem. A* 2021, **9**, 4984-4989.